Exhibit C.

RF/MICROWAVE CIRCUIT DESIGN FOR WIRELESS APPLICATIONS

Ulrich L. Rohde
Synergy Microwave Corporation

David P. Newkirk
Ansoft Corporation

A WILEY-INTERSCIENCE PUBLICATION
JOHN WILEY & SONS, INC.
New York / Chichester / Weinheim / Brisban / Singapore / Toronto

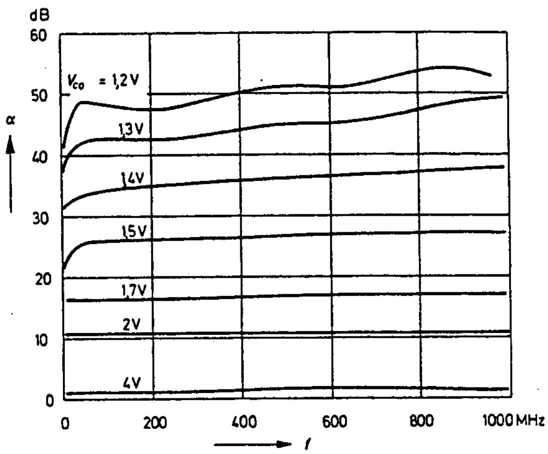

Figure 2-30 Attenuation versus frequency.

CHARACTERISTICS IN THE TEST CIRCUIT (FIGURE 2-28) AT T_{amb} = 25 °C

Voltage for 1% cross-modulation	V_{cr}	1	V
Attenuation in the 40–1000-MHz range:			
At V_{co} = 1.5 V (1–2 V)	a_{max}	45 (> 36)	dB
At V_{co} = 5 V (4–5 V)	a_{min}	1.5 (< 2)	dB
Reflection coefficient in the 40–1000-MHz range over the entire control range, depending on circuit design	a_{refl}	20 (> 16)	dB

These data reveal that the compact design of the three PIN diodes in a common 50B4 plastic package guarantees favorable values for minimum and maximum attenuation, as well as reflection attenuation. The test and application circuit shown in Figure 2-28 also comprises the transistor control-signal amplifier. The typical characteristic of the attenuation and the reflection attenuation for this circuit are shown in Figure 2-29, as a function of the control voltage V_{co}. Figure 2-30 shows the attenuation at different control voltages, as a function of frequency.

2-1-4 Tuning Diodes

Introduction. In recent years, continuous development of tuning diodes—also known as *varactors* or *varicaps*—together with increased commercial and military use has led to substantial improvement in Q, reproducibility, and reliability. Concurrently, new techniques for producing and controlling a hyperabrupt dopant profile in the semiconductor permit the capacitance–voltage law to be much faster than the classical square root or cube root behavior.

Current tuning diode materials include silicon and gallium arsenide; silicon is favored for low cost and lower Q applications from HF through microwave frequencies. Hyperabrupt varactors, also of silicon, are finding many applications in commercial television tuners, where their high tuning ratios, linear tuning, and low cost are needed. New developments include low-capacitance hyperabrupts for microwave and wireless applications.

Post-tuning drift can be characterized as short-term and long-term. Short-term PTD occurs in the time range of tens of nanoseconds to a few seconds, while long-term PTD occurs in the time range of seconds to minutes, hours, or days.

Short-term PTD is mainly dependent on the thermal properties of the diode and is improved by high Q (low power loss) and flip chip construction. Long-term PTD depends on oxide stability and freedom of mobile charge in the oxide. It should be noted that actual oscillation frequency change may occur even with a perfect tuning diode because of variation with frequency in the power dissipated by the diode, changes in the diode heat-sink temperature, and frequency changes due to other circuit elements. Less than 0.01% short- and long-term PTD can be obtained.

Distortion Products. Inasmuch as nonlinear components generate harmonics and other distortion products, an understanding of this mechanism is of prime interest to the circuit designer. In some instances, the distortion products are the desired end result of the circuit design, as in frequency multipliers, where harmonics of the input signal frequency are the required output signal. For other applications, such as tuning-diode-tuned linear circuits, distortion products are extremely undesirable, and in some instances the end product specification may set a maximum limit on the distortion products allowed.

Cross-Modulation. Cross-modulation is the transfer of the modulation on one signal to another signal and is caused by third-order and higher odd-order nonlinearities in the behavior of the device. Rewriting Eq. (2-42) we have

$$C(V) = \frac{C_0}{(1 + V/\varphi)^n} \tag{2-52}$$

where C_0 = capacitance
V = applied voltage = $V_0 + v$
V_0 = dc applied voltage
v = ac applied voltage

Then, for a desired signal of

$$S_1 = v_1 \sin \omega_1 t \tag{2-53}$$

and a second, amplitude-modulated signal of

$$S_2 = v_2(1 + m \cos \omega_m t)\sin \omega_2 t \tag{2-54}$$

it can be shown that the cross-modulation, γ, defined by

$$\text{Output signal} \sim v_1 \sin \omega_1 t + \gamma \sin (\omega_1 \pm \omega_m)t \tag{2-55}$$

is found to be

From this equation it c

- Proportional to th
- Directly proporti
- Independent of th
- Independent of th nonlinearity to wl so this is the case
- Present for all va

Solving Eq. (2-56) for we have

The interfering signa modulated interfering diode are shown in Fi

From this figure, it c cross-modulation thar

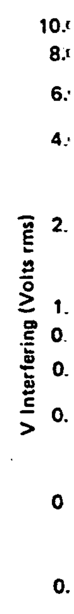

Figure 2-43 Interfering for abrupt-junction and h

$$\gamma = \frac{n(n+1)m v_2^2}{4(V_0+\varphi)^2} \tag{2-56}$$

From this equation it can be seen that cross-modulation is:

- Proportional to the square of the interfering signal
- Directly proportional to the interfering signal's modulation index, m
- Independent of the strength of the desired signal
- Independent of the frequencies of the desired and interfering signals (assuming that the nonlinearity to which both signals are subjected is sufficiently frequency-indiscriminate so this is the case)
- Present for all values of n; that is, no value of n gives zero cross-modulation UNAVOIDABLE

Solving Eq. (2-56) for the signal level v_2 required to produce cross-modulation of value γ, we have

$$v_2 = \frac{2(V_0+\phi)\gamma}{n(n+1)^m} \tag{2-57}$$

The interfering signal levels required to produce 1% cross-modulation from a 30%-modulated interfering signal applied to an abrupt-junction diode and a hyperabrupt-junction diode are shown in Figure 2-43.

From this figure, it can be seen that the hyperabrupt-junction diode is more susceptible to cross-modulation than the abrupt-junction diode in the region of maximum slope of the

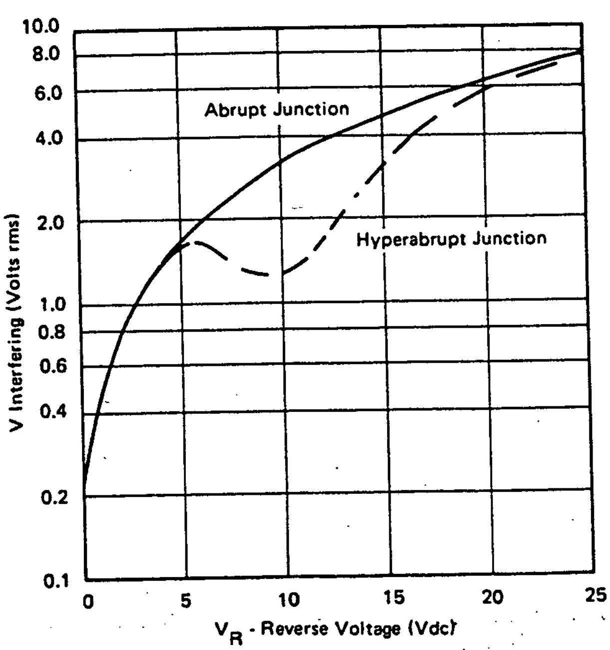

Figur 2-43 Interfering signal (30% amplitud modulated) level versus bias for 1% cross-modulation for abrupt-junction and hyperabrupt-junction diodes.

hyperabrupt-junction diode. For many applications, however, distortion products will be generated by other devices, such as transistors, at signal levels considerably below those given in Figure 2-43.

Intermodulation. Intermodulation is the production of undesired frequencies in the form

$$\sin(2\omega_1 t - \omega_2 t) \quad \text{and} \quad \sin(\omega_1 t - 2\omega_2 t) \tag{2-58}$$

from an input signal in the form of

$$v(\cos \omega_1 t + \cos \omega_2 t) \tag{2-59}$$

From an analysis similar to that done for cross-modulation, it can be shown that

$$\text{Intermodulation} = \frac{n(n+1)v^2}{8(V_0 + \varphi)^2} \tag{2-60}$$

or

$$\text{Cross-modulation} = (2m) \times \text{Intermodulation} \tag{2-61}$$

Harmonic Distortion. Harmonic distortion products are integral multiples of the signal frequencies and decrease in amplitude as the harmonic number decreases. Due to passband considerations and amplitude decrease with harmonic number, the second harmonic is the one of prime concern. Again, it can be shown that the second harmonic, v_2, of a signal of amplitude v_1 is

$$v_2 = \frac{n}{3(V_0 + \phi)} v_1^2 \tag{2-62}$$

Figure 2-44 shows the signal level required to produce 10% second-harmonic distortion in an abrupt-junction and a hyperabrupt-junction diode. Again, as in the case of cross-modulation, the hyperabrupt-junction diode is slightly worse than the abrupt-junction diode in the region of maximum slope of the hyperabrupt-junction diode.

Reduction of Distortion Products. In some cases, the signal levels applied to the diode generate distortion products larger than desirable for the circuit application. In this case, significant reduction in the distortion products can be achieved by using two diodes in a back-to-back configuration, as shown in Figure 2-45. Analysis shows that the fundamental signal components through the diodes are in phase and add, while some distortion products are out of phase and cancel, thus improving distortion performance.

Since the gradient of the electrical field produced in the depletion layer by a reverse bias applied to the device is proportional to the space charge density, the following equations can be written for the junction width W as a function of the reverse bias V_R:

For an Abrupt *pn* Junction (Alloyed Diodes)

$$W = \sqrt[2]{2\frac{\varepsilon_r \varepsilon_0}{q}\left(\frac{1}{C_p} + \frac{1}{C_n}\right)(V_R + V_D)} \tag{2-63}$$

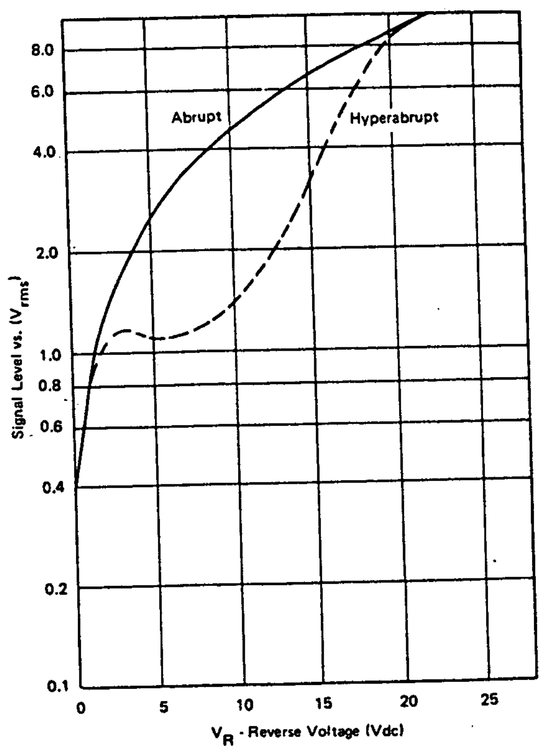

Figure 2-44 Signal level versus reverse voltage for 10% harmonic distortion.

For Linear *pn* Junctions (Single-Diffused Diodes, such as BA110–BA112)

$$W = \sqrt[3]{12 \frac{\varepsilon_r \varepsilon_0}{aq} (V_R + V_D)} \tag{2-64}$$

where a is the impurity gradient within the depletion layer, ε_0 is the absolute dielectric constant ($8.85 \times 10^{-14}\, A_s/V_{cm}$, and $\varepsilon_r \approx 12$, the relative dielectric constant of silicon.

The junction capacitance, which is inversely proportional to the junction width, therefore varies in alloyed diodes with the square root, and in single-diffused diodes with the cube root of the externally applied reverse bias, and can be calculated from the general equation

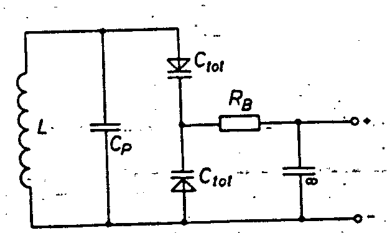

Figure 2-45 Back-to-back diodes. C_P is a fixed parallel capacitance, R_B is a bias decoupling resistor, and the capacitor marked ∞ is a low-impedance bypass.

$$C = \frac{\varepsilon_r \varepsilon_0 S}{W} \tag{2-65}$$

where S is the surface area of the pn junction. By way of approximation, we can also use the equation

$$C = \frac{K}{(V_R + V_D)^n} \tag{2-66}$$

where all constants and all parameters determined by the manufacturing process are contained in K. The exponent n is a measure of the slope of the capacitance/voltage characteristics and is 0.5 for alloyed diodes, 0.33 for single-diffused diodes, and (on average) 0.75 for tuner diodes with a hyperabrupt pn junction. Figure 2-46 shows the capacitance/voltage characteristics of an alloyed, a diffused, and a tuner diode.

Recently, an equation has been indicated which, although purely formal, describes the practical characteristics better than Eq. (2-66):

$$C = C_0 \left(\frac{A}{A + V_R} \right)^m \tag{2-67}$$

where C_0 is the capacitance at $V_R = 0$, and A is a constant whose dimension is a voltage. The exponent m is much less dependent on voltage than the exponent n in Eq. (2-66).

Equations (2-63) through (2-67) express the pure junction capacitance of the capacitance diode, but to this must still be added a constant capacitance, determined by structure parameters, in order to obtain the diode capacitance C_{tot}, which interests the user. With high inverse voltages—that is, low junction capacitance—a difference will therefore arise between the theoretical capacitance/voltage characteristic according to Eq. (2-66) and the practical characteristic, as shown in Figure 2-47.

The operating range of a capacitance diode or its useful capacitance ratio

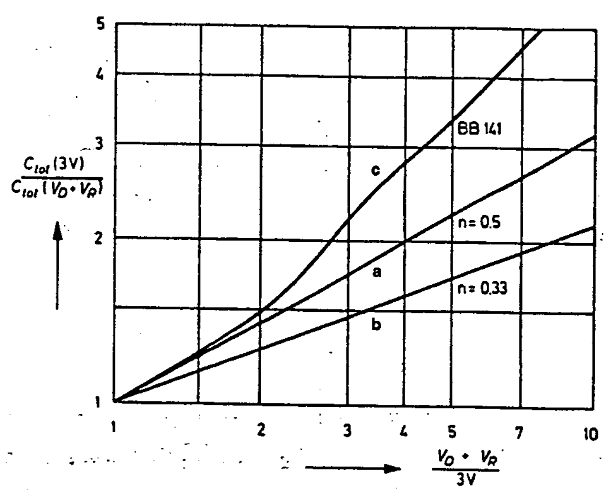

Figure 2-46 Capacitance/voltage characteristic for (a) an alloyed capacitance diode, $n = 0.5$; (b) a diffused capacitanc diode, $n = 0.33$; and (c) a wide-range tuner diode (BB141).

$$\frac{df}{f} = -\frac{1}{2}\frac{dC_0}{C_0} - \frac{1}{2}\frac{d(L-L_0)}{L} - \frac{1}{2}\frac{dL_0}{L_0} + \frac{n}{2}\frac{dV_R}{V_R+V_D} \tag{2-90}$$

The spread of parameters dC_0/C_0 and dL_0/L_0 can only be compensated by varying the circuit inductances $d(L-L_0)/L$ or by varying the bias $dV_R/(V_R+V_D)$.

Modulating the Diode Capacitance by the Applied ac Voltage. In normal operation, the sum of the tuning voltage and the alternating signal voltage of the resonant circuits is applied to the tuner diode. The bias, and thus the capacitance, of the tuner diode therefore varies at the rhythm of the alternating voltage. Due the nonlinear character of the capacitance versus voltage curve, voltage distortions and capacitance shifts are inevitable, and these must be kept within adequate limits. This is done by maintaining the ac applied to the diode(s) at sufficiently low ac amplitude and by choosing an adequate minimum value for the tuning voltage. In the resonant circuit, a tuner diode is modulated predominantly by a current free from harmonics, according to the equation

$$i = \hat{i}\cos\omega t \tag{2-91}$$

The alternating voltage across the diode is

$$v = (V_R + V_D)\left[\left(1 + \frac{\hat{i}(1-n)}{\omega C_{tot} V_R}\sin\omega t\right)^{1/(1-n)} - 1\right] \tag{2-92}$$

An evaluation of this equation shows that especially the first harmonic makes its appearance. The capacitance shift caused by the alternating voltage superimposed on the tuning voltage is shown in Figure 2-63. However, the voltage distortion, and thus the capacitance shift, can be largely avoided if two tuner diodes are used, as in Figure 2-61.

COMPENSATING TEMPERATURE DEPENDENCE. As has already been mentioned, variations are caused in the capacitance of the diode mainly by the dependence of the diffusion voltage on

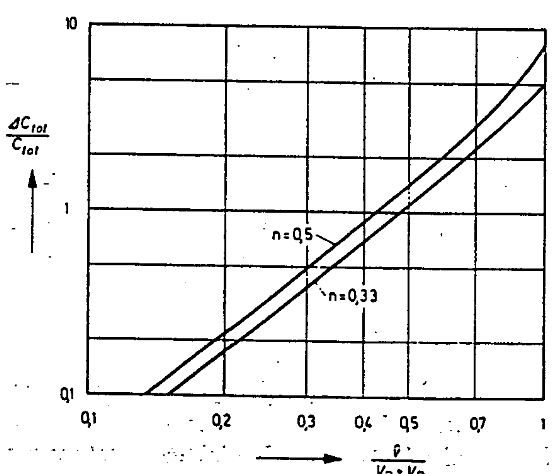

Figur 2-63 Capacitance increas as a function of the ac voltage drop across the tuner diode.

mperature. In a dio
equency, therefore,
erefore impossible
means of tempera
cally tuned circuits.
To achieve satisfac
equal to that by whic
that is, by approxima
silicon diode in serie
the forward voltage

which determines th
almost temperature i
current via the resist
to prevent capacitiv
To prevent the lo
ctuating in a man
65 may be used i
d the only load
transistor.

ynamic Stability.

3-6 A NOVEL APPROACH TO VOLTAGE-CONTROLLED TUNED FILTERS INCLUDING CAD VALIDATION [28]

Modern receivers control input stages as well as the oscillator band and frequency by electrical rather than mechanical means. Tuning is accomplished by voltage-sensitive capacitors (varactor diodes), and band switching by diodes with low forward conductance. Since the wireless band (essentially 400 MHz to 2.4 GHz) is so full of strong signals, the use of a tracking filter is desired as a solution to improve the performance and prevent second-order IMD products or other undesired overload effects. The dc control voltage needed for the filter can easily be derived from the VCO control voltage. There may be a small dc offset, depending on the IF used.

3-6-1 Diode Performance

The capacitance versus voltage curves of a varactor diode depend on the variation of the impurity density with the distance from the junction. When the distribution is constant, there is an "abrupt junction" and capacitance follows the law

$$C = \frac{K}{(V_d + V)^{1/2}} \tag{3-183}$$

where V_d is the contact potential of the diode and V is applied voltage.

Such a junction is well approximated by an alloyed junction diode. Other impurity distribution profiles give rise to other variations, and the above equation is usually modified to

$$C = \frac{K}{(V_d + V)^n} \tag{3-184}$$

where n depends on the diffusion profile and $C_0 = K/V_d^n$.

A so-called graded junction, having a linear decrease in impurity density with the distance from the junction, has a value of n. This is approximated in a diffused junction.

In all cases these are theoretical equations, and limitations on the control of the impurity pattern can result in a curve that does not have such a simple expression. In this case, the coefficient n is thought of as varying with voltage. If the impurity density increases away from the junction, a value of n higher than 0.5 can be obtained. Such junctions are called hyperabrupt. A typical n value for a hyperabrupt junction is about 0.75. Such capacitors are used primarily to achieve a large tuning range for a given voltage change. Figure 3-144 shows the capacitance–voltage variation for the abrupt and graded junctions as well as for a particular hyperabrupt-junction diode. Varactor diodes are available from a number of manufacturers, such as Motorola, Siemens, and Philips. Maximum values range from a few to several hundred picofarads, and useful capacitance ratios range from about 5 to 15.

Figure 3-145 shows three typical circuits that are used with varactor tuning diodes. In all cases, the voltage is applied through a large resistor R_e or, better, an RF choke in series with a small resistor. The resistance is shunted across the lower diode and may be converted to a shunt load resistor across the inductance to estimate Q. The diode also has losses that may result in lowering the circuit Q at high capacitance, when the frequency is sufficiently high. This must be considered in the circuit design.

the pair in series, and q is the charge transferred through the pair in series. This notation results in

$$\frac{v}{V'} \equiv \frac{v_1 - v_2}{V'} = \left(1 - \frac{q}{Q'}\right)^{1/(1-n)} - \left(1 - \frac{q}{Q'}\right)^{1/(1-n)} \tag{3-189}$$

For all n, this eliminates the even powers of q, and hence the even harmonics. This can be shown by expanding Eq. (3-189) in a series expansion and performing term by term combination of the equal powers of q. In the particular case $n = \frac{1}{2}$, $v/V' = 4q/Q'$, and the circuit becomes linear.

The equations hold as long as the absolute value of v_1/V' is less than unity, so that there is no conduction. At the point of conduction, the total value of v/V' may be calculated by noting that when $v_1/V' = 1$, $q/Q' = -1$, so $q_2/Q' = 1$, $v_2/V = 3$, and $v/V = -4$. The single-diode circuits conduct at $v/V' = -1$, so the peak RF voltage should not exceed this. The back-to-back configuration can provide a fourfold increase in RF voltage handling over the single diode. For all values of n, the back-to-back configuration allows an increase in the peak-to-peak voltage without conduction. For some hyperabrupt values of n, such that $1/(1 - n)$ is an integer, many of the higher-order odd harmonics are eliminated, although only $n = \frac{1}{2}$ provides elimination of the third harmonic. For example, $n = \frac{2}{3}$ results in $1/(1 - n) = 3$. The fifth harmonic and higher odd harmonics are eliminated, and the peak-to-peak RF without conduction is increased eightfold; for $n = \frac{3}{4}$ the harmonics 7 and above are eliminated, and the RF peak is increased 16 times. It must be noted in these cases that the RF peak at the fundamental may not increase so much, since the RF voltage includes the harmonic voltages.

Since the equations are only approximate, not all harmonics are eliminated, and the RF voltage at conduction, for the back-to-back circuit, may be different from that predicted. For example, abrupt-junction diodes tend to have n of about 0.46–0.48 rather than exactly 0.5. Hyperabrupt junctions tend to have substantial changes in n with voltage. The diode illustrated in Figure 3-144 shows a variation from about 0.6 at low bias to about 0.9 at higher voltages, with wiggles from 0.67 to 1.1 in the midrange. The value of V_d for varactor diodes tends to be in the vicinity of 0.7 V.

3-6-2 A VHF Example

The application of tuning diodes in double-tuned circuits in TV tuners has been common practice for many years. Figure 3-146 shows the circuit diagram. The input impedance of 50 Ω gets transformed up to 10 kΩ. The tuned circuits consist of the 0.3-μH inductor and two sets of antiparallel diodes. By dividing the RF current in the tuned circuit and using several diodes instead of just one pair, intermodulation distortion is reduced.

The coupling between the two tuned circuits is tuned via the 6-nH inductor that is common to both circuits. This type of inductance is usually printed on the circuit board. The diode parameters used for this application were equivalent to the Siemens BB515 diode. The frequency response of this circuit is shown in Figure 3-147.

The coupling is less than critical. This results in an insertion loss of about 2 dB and relatively steep passband sides. Once the circuit's large-signal performance (Figure 3-148) is seen, a third-order intercept point of about −2 dBm is not so unexpected. The reason for this poor performance is the high impedance (high L/C ratio), which provides a large RF voltage swing across the diodes. A better approach appears to be using even more diodes and at the same time changing the impedance ratio (L/C ratio).

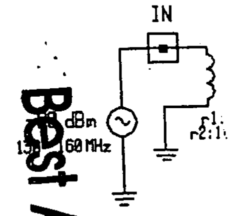

Figur 3-146 Double-
parallel diodes, the IMC

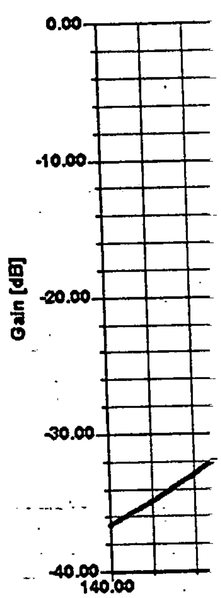

Figur 3-147 Frequ
(less than transitiona

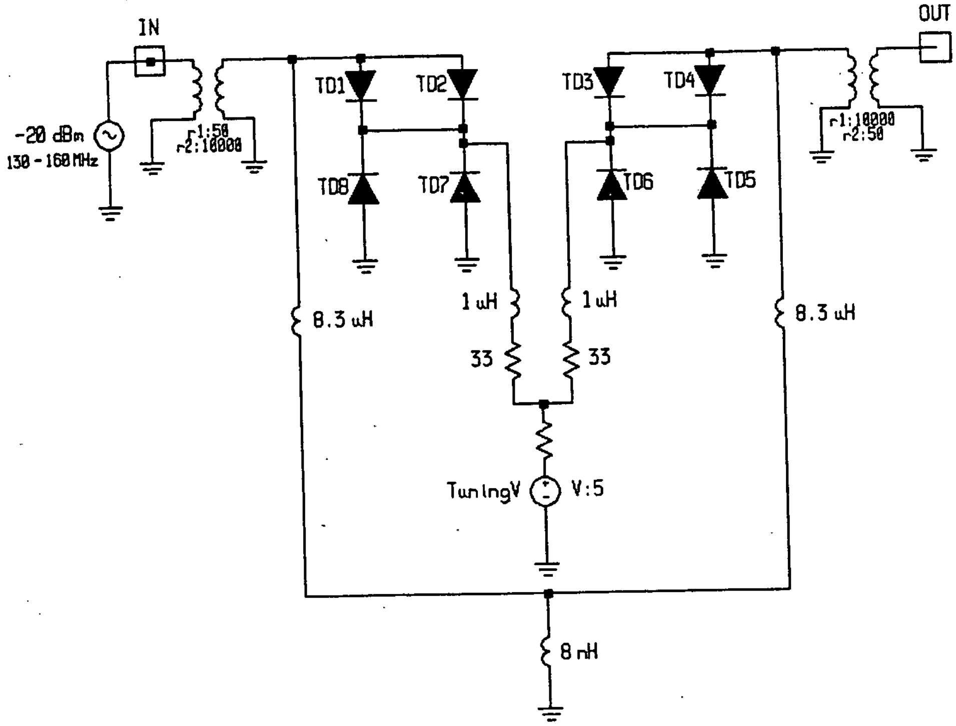

Figur 3-146 Double-tuned filter at 161 MHz using hyperabrupt-junction tuning diodes. By using several parallel diodes, the IMD performance improves.

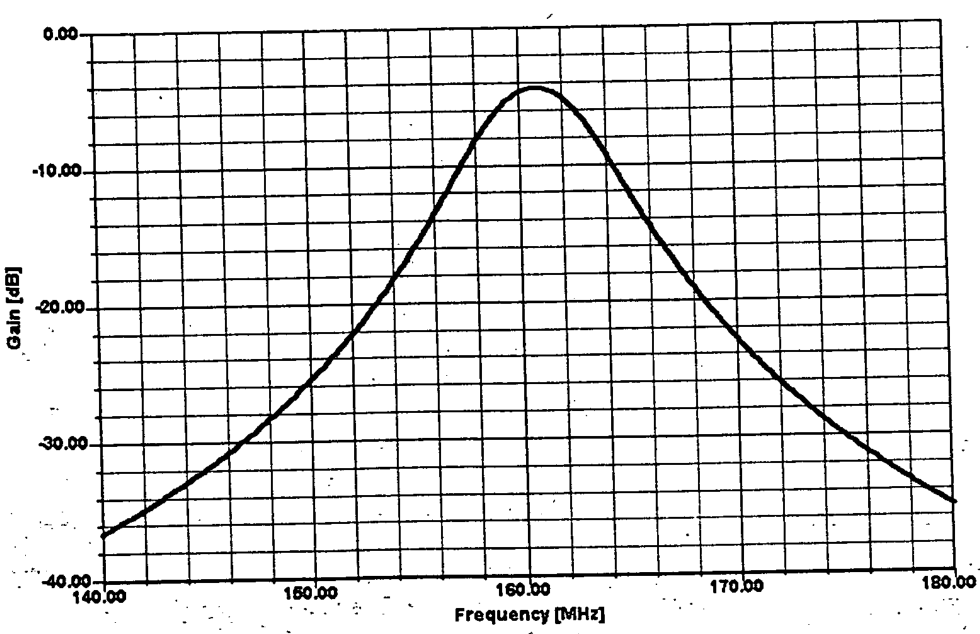

Figure 3-147 Frequency response of the tuned filter shown in Figure 3-146. The circuit is undercoupled (less than transitional coupling); $Q \times k < 1$.

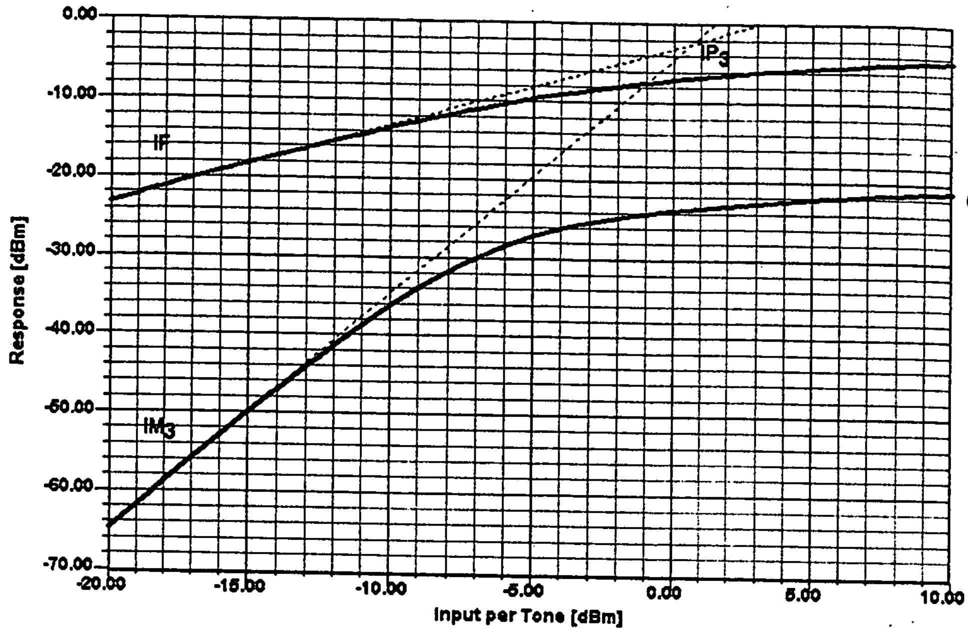

Figure 3-148 Prediction of intercept point of the double-tuned circuit shown in Figure 3-146. Note the compression of both the input signal and the IMD product.

3-6-3 An HF/VHF Voltage-Controlled Filter

The above example used a step-up procedure typically done by a tap at the input and output inductance. This method allows an impedance transformation; however, if one desires to change it into a series-tuned arrangement, it has to be done with a transformer. The large-signal conditions in the frequency range from 10 to 30 MHz on a medium- to large-sized antenna are equivalent to, if not worse than, the conditions for VHF operation. The only exception would be line of sight into the transmitter such as a tower in the middle of the city. Examples of such hostile conditions would be any large city, such as Munich, New York, Miami, Chicago, and San Francisco, where the authors had significant experience with intermodulation distortion problems.

By translating the circuit into a low-impedance-drive arrangement, building it symmetrically, and reducing the tuning range somewhat by capacitors and many series diode pairs, the filter's large-signal performance was significantly improved. The tuning diodes had about 125 pF at 1 Vdc per unit. Initial tests trying to use a high-capacitance diode, such as the BB112, resulted in much higher IMD products. The B112 has a 1-V capacitance of 470 pF down to about 20 pF at 8 V. Standard diodes show about 30 pF at 1 V, while the diodes used in the experiment had a 125-pF capacitance at 1 V. These experimental diodes were made available from a well-known manufacturer for this evaluation. Figure 3-149 shows the circuit diagram.

A step-down transformer drives the tuned circuit with a source impedance of 12.5 Ω. The circuit is symmetrical. There are two 0.8-μH inductors and 2 × 5 diodes in the loop. The output of the circuit is transformed back up to 50 Ω. The tuning voltage is supplied via a heavily filtered arrangement. This circuit has actually been implemented in Rohde & Schwarz field strength meter equipment. They guarantee an intercept point of about +20 dBm. The selectivity of these circuits is quite reasonable and mostly intended to reduce

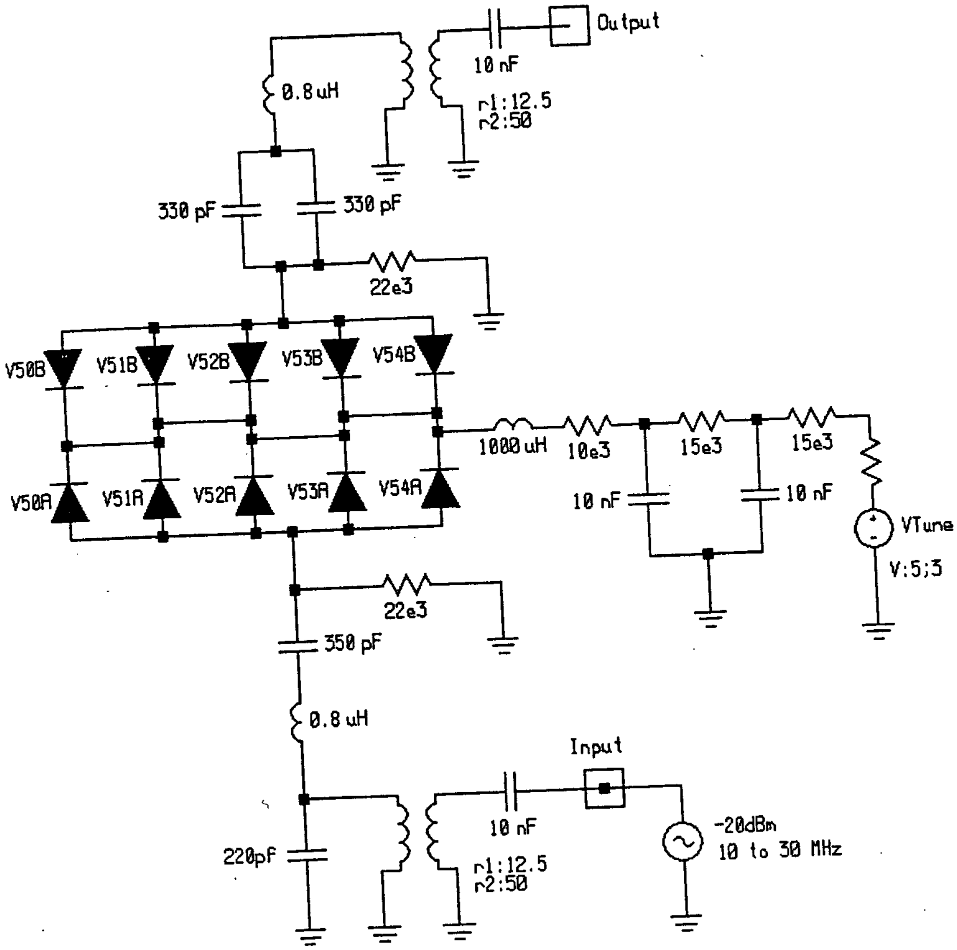

Figure 3-149 High dynamic range of a 10–20-MHz filter.

second-order intermodulation distortion products by about 10 dB, at the same time having a high third-order intercept point. Figure 3-150 shows the selectivity curves at two different tuning voltages.

The most interesting number, however, is the third-order intercept point (already determined as about 20 dBm), which still had to be simulated. This sometimes sounds like a contradiction: Once the measured values are available and are acceptable, why would one want—or, rather, need—to do a simulation besides the necessity to develop a high-input intercept filter? It was desirable to validate the nonlinear models and prove that the above-mentioned equations will hold true. This type of simulation is now more difficult because the number of nonlinear elements went from four to ten, and some numerical problems, such as convergence difficulties, can be expected, and the effect of harmonic frequency cancellation (compensation) can also be seen. By using diode combinations that result in $1(1 - n)$, n being an integer number, these IMD products can drastically be reduced. This implies that each of the five diode pairs has a selected value for n to meet this condition. Later, a final attempt will be made to improve the first VHF filter with the proper diode combinations.

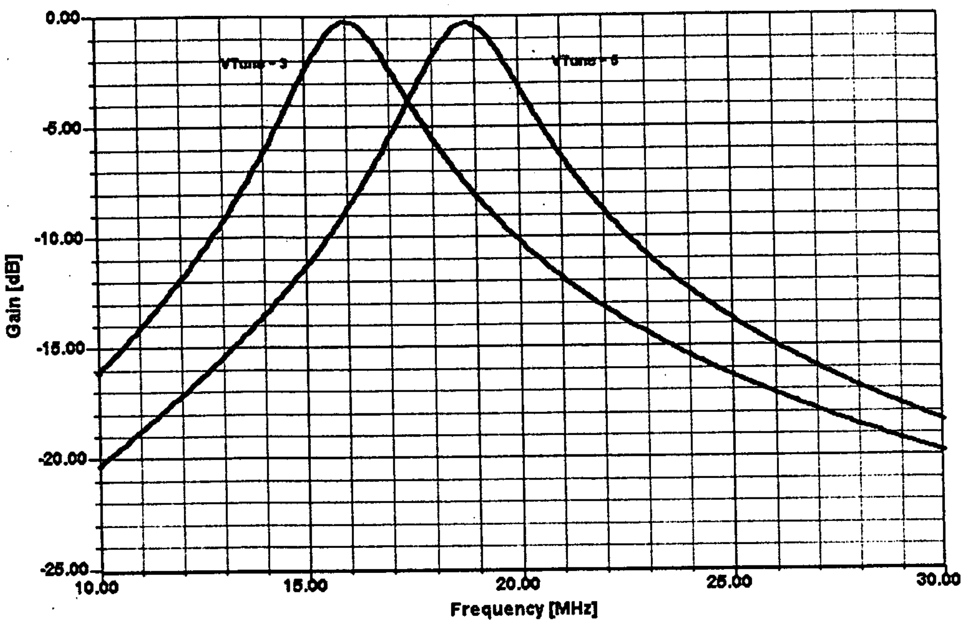

Figure 3-150 Frequency response of the filter shown in Figure 3-149. Filters of this type are intended to reduce second-order IMD by providing about 20-dB suppression at half the center frequency.

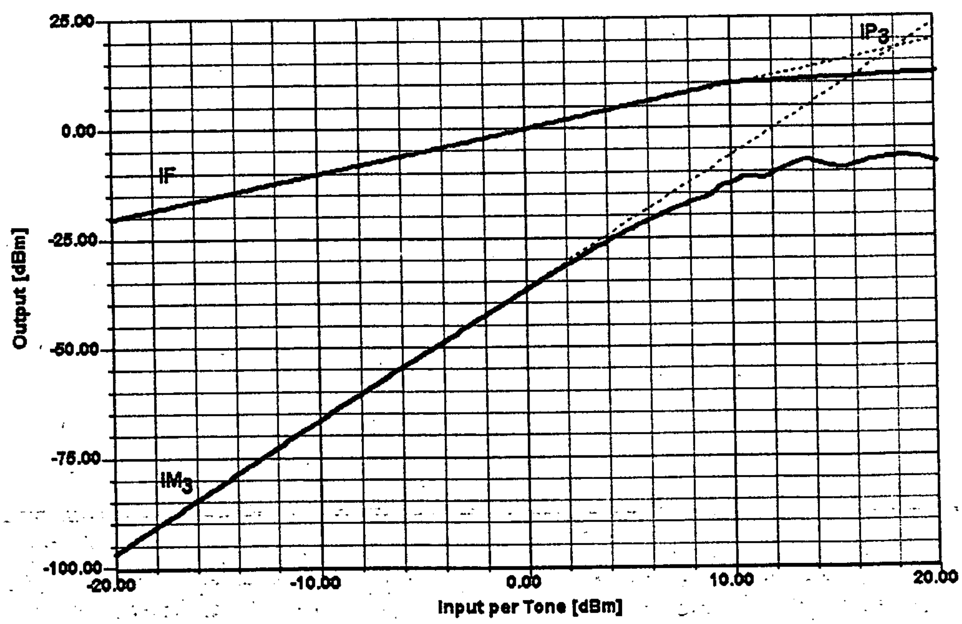

Figure 3-151 Prediction of third-order intercept point of the filter shown in Figure 3-149. The reason for the curves on the IMD plot lies in the interaction between the ten nonlinear devices.

Figure 3-151 show
shown in Figure 3-14
selection and measure
compared to the meas
the diodes' voltage-de
performance and the
mentioned earlier, has
was probably the fir
improved performanc

3-6-4 Improving

By selecting the appr
3-152, a significant I
special shunt arrang
which allows its val
showed an improve
maintained. Figure 3
coupling slightly gre

3-6-5 Conclusic

After explaining so
examples of voltage
has also shown tha
circuits.

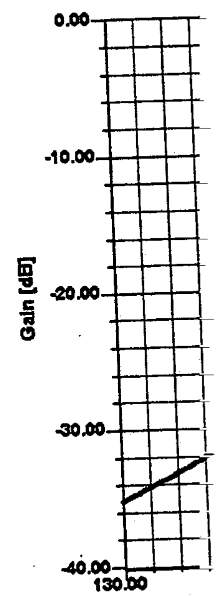

Figur 3-152